Dynamics of melting argon clusters

Gayle M. Tanner,[1,2] Aniket Bhattacharya,[1] Saroj K. Nayak,[3] and S. D. Mahanti[1]
[1]*Department of Physics, Michigan State University, East Lansing, Michigan 48824-1116 and Center for Fundamental Material Research, East Lansing, Michigan 48824-1116*
[2]*Department of Physics, Oregon State University, Corvallis, Oregon 97331*
[3]*Physics Department, Virginia Commonwealth University, Richmond, Virginia 23284-2000*
(Received 22 August 1996)

With increasing total energy, small atomic clusters show a *smooth* transition from a rigid solidlike to a floppy liquidlike ''phase.'' In certain clusters, depending on their structure and stability, this transition takes place over a finite energy range where both these ''phases'' coexist in a dynamical sense, whereas in others the transition does not involve a coexistence region and has been called ''slushlike.'' Previous studies in Ar_{13}, which belongs to the first kind, have established the energy variation of maximal Lyapunov exponent (MLE) and the dynamic structure factor (DSF) as ''dynamical indicators'' of this transition. To understand the general features of these dynamic indicators better, we investigated the dynamic properties of two clusters Ar_{19} and Ar_{17}. The former is a magic number cluster whose behavior is expected to be similar to Ar_{13}, whereas the latter which does not show a coexistence region belongs to the second kind. Ar_{19} shows a behavior similar to Ar_{13}. In Ar_{17}, we find that above the transition but close to it, the DSF still shows features exhibiting the interplay of a ''hot solid''and a ''cold liquid'' as observed in the coexistence region of Ar_{13} and Ar_{19}. Unlike the bond length fluctuation which exhibits a rapid increase near the transition, the behavior of MLE is rather smooth and it does not serve as a good dynamical indicator of the transition in the Ar_{17} system. [S1063-651X(97)13601-7]

PACS number(s): 05.70.Fh, 36.40−c, 64.60.My, 64.70.Dv

I. INTRODUCTION

During the last decade, there has been a great deal of interest in studying very small, nanometer to subnanometer scale, aggregates of particles because their properties are significantly modified from those of bulk materials [1]. Examples are atomic and molecular clusters containing a small number of particles. As compared to the bulk, a distinct feature of the clusters, particularly of the small ones, is that the local environment can vary dramatically from one atom to the other. This results in inhomogeneities on different length scales. One expects to see the effects of this inhomogeneity in their dynamical properties, as one heats a cluster from its ground state through the temperature region where it changes from a rigid solidlike to a floppy liquidlike ''phase,'' referred to loosely as the melting of a cluster [2].

The dynamics of a small cluster as it makes excursions through different pathways in phase space can be seen through molecular dynamics simulation. Such studies go back to the earlier work of Briant and Burton [3], which has been extended very thoroughly in a series of papers by Berry and co-workers [2]. The major outcome of these simulation studies is that the melting of clusters is quite unique. The short-time averages of the kinetic energy of some clusters, e.g., Ar_{13}, shows a *bimodal* distribution in a finite energy range $E_f \leqslant E \leqslant E_m$. This implies that, instead of showing a coexistence of two phases in contact at a given time, there is a dynamical coexistence of a ''hot'' solidlike phase and a ''cold'' liquidlike phase in the above energy range. In this energy range the cluster makes dynamic excursions between two distinct regions of phase space with different characteristics, solidlike and liquidlike. More recently it has been shown by Nayak, Ramaswamy, and Chakravarty [4] that the signature of the onset of this transition is clearly seen in a dramatic increase in the maximal Lyapunov exponent (MLE) near E_f. In a subsequent paper they also established the presence of $1/f^{\alpha}$ noise in the power spectra of the potential energy fluctuation of a 'tagged' particle [5] when the cluster goes into the liquidlike state. Although a careful analysis of the energy dependence of the exponent α across the transition region has not been carried out, it appears that this exponent is weakly energy dependent in the transition region, and starts to decrease rapidly as one enters the liquid phase (characterized by a unimodal distribution of short-time averages of potential and kinetic energies). As pointed out by Nayak, Ramasyamy, and Chakravarty, this exponent should be zero, i.e., the correlations are δ correlated in time, in the liquid state. However it appears that for clusters, particularly the small ones, one has to go to very high temperatures to approach this limiting behavior.

Except at very small excitation energies, the classical dynamics of clusters is chaotic, and it has been rightly studied previously by looking at the clusters as chaotic dynamical systems [6]. The presence of $1/f^{\alpha}$ noise in the power spectrum of potential energy fluctuation of a tagged particle as the cluster enters the coexistence region reflects a temporal scale invariance, which is seen over a large range of frequency. The origin of this power law spectra is the strong correlations existing over times spanning several orders (about 3) of magnitude. Experimental indications of phase change in clusters are still indirect, and there is a strong need for experimental signatures for solid-liquid transitions in clusters. Since melting transitions are usually associated with a structural rearrangements, one expects the frequency (ω)- and wave-vector (k)-dependent dynamic structure factor (DSF) $S(k,\omega)$ of the cluster to reflect the characteristic

features associated with solidlike and liquidlike phases, and in particular existing long-time correlations. In addition, by changing k, or equivalently the length scale over which the dynamics is probed, one can expect to see the inhomogeneous nature of the cluster. Molecular dynamics (MD) simulation results on an Ar_{13} cluster indeed show that the DSF can be used as a very efficient tool to probe cluster melting [7]. We should point out that inelastic neutron scattering cross section is directly proportional to the self-part of the DSF giving further motivation to carry out a careful study of this quantity using MD simulations.

In this paper we make a detailed study of the dynamics of Ar_{19} and Ar_{17} clusters by calculating both the DSF and MLE to see if indeed there are any correlations between these two dynamic indicators. While the caloric curve for Ar_{19} is similar to that for Ar_{13}, indicating a finite energy coexistence region for the former, the one for Ar_{17} exhibits a ''slushlike'' behavior resulting from its loosely bound structure [8]. We therefore expect to see a rapid increase in the MLE at the onset of the coexistence region, and characteristics of solid-liquid coexistence in the DSF for Ar_{19} similar to that seen in Ar_{13} [4,7]. On the other hand, it is not obvious how MLE and DSF should behave in the case where the solid-liquid transition is smooth, and there is no coexistence region as in the slushlike transition seen in Ar_{17}. Do the DSF and MLE still remain as good ''dynamical indicators'' of this transition? Recently Mehra and Ramaswamy [9] suggested that MLE should show a knee in its energy dependence near a continuous transition. Thus if the transition in Ar_{17} is indeed smooth and there is no energy range over which the solidlike and the liquidlike phases coexist dynamically, then MLE should show a knee rather than a rapid increase near the transition [9]. Previous studies of another model exhibiting continuous phase transition also exhibited a ''knee'' [10]. It is not clear what DSF should show in such a situation. These are some of the questions we address in this paper taking Ar_{17} as a prototype of all these clusters which do not form closed shells. The arrangement of this paper is as follows: In Sec. II we give the interatomic potential, and describe simulation methods which we used. In Sec. III, we briefly discuss previous work and define different time correlation functions which have been studied to probe the dynamics. In Sec. IV, we present and discuss our results and, finally, in Sec. V, give a brief summary.

II. COMPUTATIONAL METHOD

In our isoergic MD simulations, both the fifth order Gear predictor corrector and velocity-Verlet algorithms were used to solve Newton's equations [11–13]. DSF's and MLE's were computed using these two algorithms, respectively. The caloric curves obtained with these two simulations were, however, nearly identical. The accuracy of MD simulations is determined by the degree to which energy is conserved. Employing the Gear algorithm, the total energy deviated by at worst 0.01% using a time step of 5 fs for 2×10^5 steps, and by less than 0.001% using a time step of 2.5 fs for 1.2 million time steps. Similar accuracies were also obtained in our Verlet simulations. Starting from suitable initial configurations, the system was allowed to equilibrate for 2×10^5 time steps of $5\text{x}10^{-15}$ s at constant energy. At the end of the run, the final positions and their derivatives were stored. The cluster was then heated by scaling the velocities every 200 time steps, for 2000 time steps, increasing the total energy of the system by approximately 0.05×10^{-14} erg/atom. This resulted in a temperature (as measured by the long-time average of the kinetic energy) increase from 1–3 K, corresponding to a maximum heating rate of 3 K/ps. This follows the procedure for the proper heating of microclusters presented by Briant and Burton [3]. The MLE's were computed using the tangent space method [14]. To obtain a convergent value of the MLE, λ, we used the following procedure. At each energy, after the usual equilibration run, the equations of motion are followed for 3×10^5 MD steps and λ is obtained from the final 2×10^5 MD step trajectories. The average value of λ, computed from its values obtained from 5000 MD step segments, was found to be essentially the same as the asymptotic value indicating that a converged value of λ had been obtained.

III. PREVIOUS STUDIES

The solid-liquid transition region is generally determined by calculating the long-time averages of the kinetic energy (E_{kin}) and the rms bond-length fluctuation δ as a function of the total energy. The latter is given by

$$\delta=\frac{2}{N(N-1)}\sum_{i<j}\frac{(\langle r_{ij}^2\rangle-\langle r_{ij}\rangle^2)^{1/2}}{\langle r_{ij}\rangle}. \tag{1}$$

The temperature of the system, T, is directly related to the average kinetic energy by the relation

$$T=\frac{2}{3N-6}\frac{E_{\text{kin}}}{k_B}, \tag{2}$$

where $k_B = 1.381\times10^{-16}$ erg/K is the Boltzmann constant, and $3N-6$ represents the total number of internal degrees of freedom.

As mentioned by Beck, Jellinek, and Berry [2], short-time averages of the kinetic energy carried over several vibrational time periods display multimodal distributions for clusters undergoing melting characterized by a coexistence region. We have reproduced these features in Ar_{13} and Ar_{19}, as found in earlier studies by Berry and his collaborators.

To probe the space-time dynamics of the cluster, we calculated the incoherent intermediate scattering function

$$F_s(\vec{k},t)=\int_{-\infty}^{\infty}d\vec{r}e^{i\vec{k}\cdot\vec{r}}G_s(\vec{r},t), \tag{3}$$

where G_s(r,t), the self-part of the Van Hove correlation function, is the probability density that a particle is located in the volume element $d\vec{r}$, about a point $\vec{r}$, at time t, given that it was at the origin at $t=0$.

$$G_s(\vec{r},t)=\frac{1}{N}\left\langle\sum_{j=1}^{N}\delta(\vec{r}-[\vec{r}_j(t)-\vec{r}_j(0)])\right\rangle, \tag{4}$$

where the angular brackets $\langle\rangle$ imply an average over initial positions and times of the particles. From Eq. (3), it follows that

$$F_s(\vec{k},t)=\frac{1}{N}\left\langle \sum_{j=1}^{N} e^{i\vec{k}\cdot[\vec{r}_j(t)-\vec{r}_j(0)]}\right\rangle. \quad (5)$$

Also computed is the dynamic structure factor

$$S_s(\vec{k},\omega)=\int_{-\infty}^{\infty} dt e^{-i\omega t}F_s(k,t). \quad (6)$$

The dynamical stability of the trajectories in phase space can be probed by computing Lyapunov exponents. For an N-atom cluster, the phase is $6N$ in dimension. Since there are seven constants of motions in our constant energy simulations—three components of linear and angular momenta and the total energy—there are $6N-14$ Lyapunov exponents [15]. The maximum of these, the MLE, characterizes the fastest rate of exponential divergence of two nearby trajectories, and is given by

$$\lambda=\lim_{t\to\infty}\lim_{d(0)\to 0}\frac{1}{t}\ln\frac{d(t)}{d(0)}, \quad (7)$$

where $d(0)$ and $d(t)$ are the initial and final (after time interval t) distances between two trajectories, respectively. For chaotic dynamics, $\lambda>0$ and $\lambda=0$ is a signature of regular motion.

Thus there are several physical quantities such as δ, $F_s(\vec{k},t)$, $S_s(\vec{k},\omega)$, and λ which are expected to show characteristic changes with energy as a cluster undergoes the melting process. In Sec. IV, we report our results on these quantities for different Ar clusters.

IV. RESULTS

A. Ar_{19} and Ar_{13} clusters

As mentioned earlier, the main theme of this paper is to present some results on Ar_{19} and Ar_{17} clusters. However, first as a cross-check, we present results for an Ar_{19} cluster and see how they compare with Ar_{13}, a stable magic number cluster [4,7]. Its caloric curve is very similar to that of Ar_{13}, and one expects to see qualitatively similar behavior for both in DSF's and MLE's. Earlier studies by Jellinek, Beck, and Berry [8] for Ar_{13} and Ar_{19} have shown that general features of the dynamics of these two similar closed shell clusters can be characterized by three different energy or, equivalently, three different temperature regimes: the low energy regime ($E\leqslant E_f$) exhibiting solidlike properties, the coexistence regime ($E_f\leqslant E\leqslant E_m$) which has the characteristic of both solid and liquid, and the high energy ($E\geqslant E_m$) liquidlike regime. The short-time averages of the kinetic energy shows a bimodal distribution in the coexistence region both in Ar_{13} and Ar_{19}. For the latter system, we calculated structure factors in the three different energy regimes discussed above. The corresponding total energy values are -5.8×10^{-14} (solid), -4.85×10^{-14} (coexistence), and -4.5×10^{-14} (liquid) erg/atom respectively. Values of the wave vector k were chosen to correspond to wavelengths ranging from interparticle separation to several times the size of the cluster, which is around 3σ - 4σ, where σ is the Lennard-Jones parameter for argon (3.4 Å). Values of $k\sigma$ run from 1 to 10, or the equivalent wavelengths run from 2 to 0.2 nm. This provides an optimum range for probing the cluster dynamics in a scattering experiment.

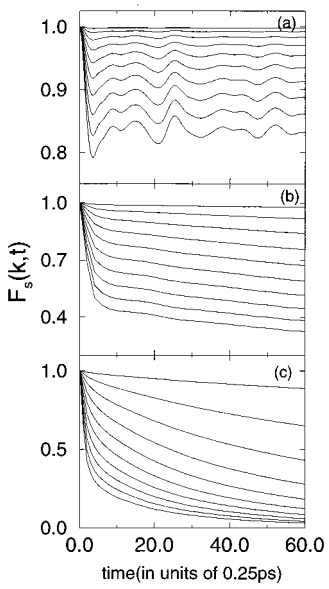

FIG. 1. $F_s(k,t)$ for Ar_{19}. (a) Solid region, $E=-5.8\times10^{-14}$ erg/atom, (b) Coexistence region, $E=-4.85\times10^{-14}$ erg/atom, (c) Liquid region, $E=-4.5\times10^{-14}$ erg/atom. For each E, $k\sigma$ = 1,2,...,10, increasing from the top to the bottom.

In Fig. 1, the time dependence of the correlation function $F_s(k,t)$ is given for several values of k. The time and k dependences of this quantity are similar to those seen in our earlier studies of an Ar_{13} cluster. In Fig. 1(a), corresponding to the rigid phase, we find that $F_s(k,t)$ shows an oscillatory time dependence, and that the amplitude of the oscillatory part increases with k, as the atoms in the rigid structure vibrate about their equilibrium positions. Since the double icosahedral structure of Ar_{19} is very stable in time, the correlations persists up to very long times. In fact it appears to saturate to a finite value as t approaches ∞, characteristics of a solid phase. This long-time asymptotic value decreases with k, a reflection of the Debye-Waller effect in solids. In contrast, in the high-energy liquidlike phase [Fig. 1(c)], the correlation function decays rapidly with time, the characteristic decay time decreases with k. There is no oscillatory behavior. For similar values of $k\sigma$, $F_s(k,t)$ in the liquid decays to a much smaller value compared to the solid in a time interval of 15 ps. For example, for $k\sigma = 10$, the correlation function has decayed nearly to zero by 15 ps in the liquid phase, whereas in the rigid phase its value is about 0.83.

In the coexistence region [Fig. 1(b)], the correlation function is clearly different from both the liquid and solid curves. The initial decay is rapid, with the $k\sigma = 10$ curve decaying to 0.5 within the first 1 ps. The function then flattens out and appears to exhibit a very slow decay which is approximately linear in time. For small and intermediate values of k, the curve appears very smooth, similar to that for a liquid, but for large k, faint oscillations resembling a solidlike dynamics show up.

In Fig. 2 the results are presented for the DSF, $S_s(k,\omega)$. We see from Eq. (5) that there is no time dependence in $F_s(k,t)$ for $k=0$, so $S_s(0,t)$ would be a δ function (with

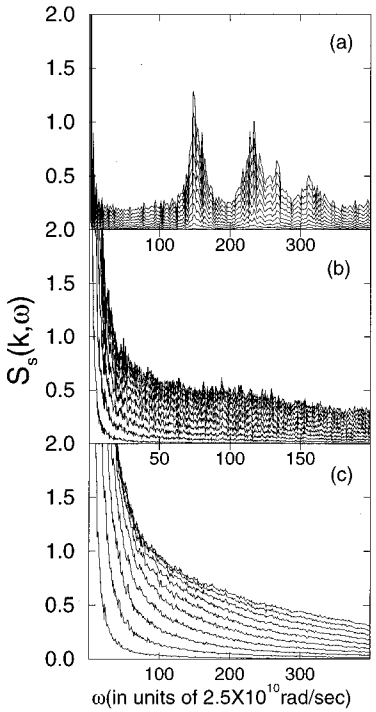

FIG. 2. $S_s(k,\omega)$ for Ar_{19} for the same set of energy and corresponding k values as in Fig. 1.

finite simulation time corrections). In the solidlike region [Fig. 2(a)], there is a very large and extremely narrow (resolution limited) central peak for all values of k. The spectral weight of this central peak decreases with k because it is proportional to the long-time limit of the correlation function. At higher frequencies, well-defined peaks are observed, corresponding to different vibrational modes of the cluster, again with their spectral weight increasing in strength with k, a characteristic feature of harmonic dynamics. [7,16] In the liquid region [Fig. 2(c)], the central peak is much more broader, and decreases much slowly at large-k values. There are no finite frequency peaks observed, as atomic motions are highly anharmonic, leading to strong damping of harmonic vibrations. In the coexistence region [Fig. 2(b)], one can clearly identify both a narrow central peak, characteristic of the solid but with a finite lifetime, and a broad structureless feature extending to higher frequencies similar to that seen in the liquid. The DSF results are almost identical (excepting for quantitative differences) to what we found for Ar_{13} [7], indicating the similarity of these two systems.

Next we discuss the MLE of Ar_{19} to see how the solid-liquid transition and the coexistence are reflected in this dynamic indicator. Shown in Fig. 3 is the energy (E) dependence of λ for Ar_{19}. At low values of E, $\lambda=0$, and it increases with E. At $E=-4.81\times10^{-14}$ erg/atom which is equivalent to $T\cong 28$ K, λ increases sharply when the cluster starts to melt. This energy lies in the coexistence region. A similar change in λ is seen when plotted as a function of T, except that in this case several values of λ fall into a small temperature interval near the transition. These different values of λ are due to the dynamical coexistence of solidlike and liquidlike phases. Here the different phases in dynamical equilibrium correspond to the cluster occupying different phase spaces in the potential energy surface: the high kinetic

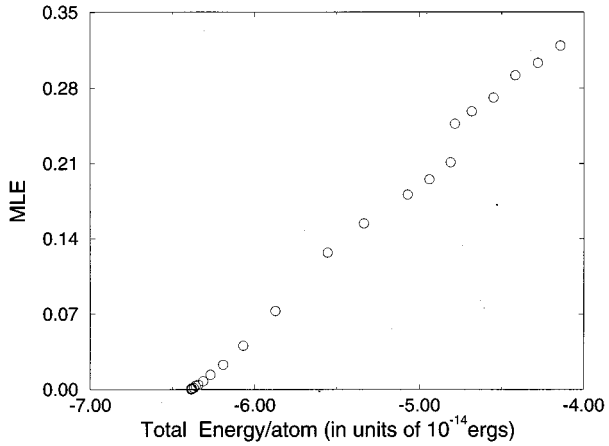

FIG. 3. Maximal Lyapunov exponent vs energy and atom for Ar_{19}.

phase (or superheated solid) corresponds to a high chaotic region, and the low kinetic phase (supercooled liquid) to a low chaotic region. This suggests that we might be able to partition the phase space into different regions using λ as an order parameter. The abrupt increase of the MLE near the transition point is due to the sudden increase of phase space volume accessible to the system. However, the change in λ depends on the nature of the transition, particularly in finite systems. For example, if the transition is abrupt (as in Ar_{13} and Ar_{19}), and the system suddenly accesses a larger volume in phase space, the change in λ is rather sharp. On the other hand, if the transition is smooth as in Ar_{17}, which will be discussed later, then λ is expected to change smoothly. It is noted here that in the bulk where the transition is sharp and there is a single energy (and T) at which the solid and liquid phases coexist, λ shows an abrupt change near the transition temperature [17]. For a cluster to exhibit a well-defined solid-liquid dynamic equilibrium and two well-defined phases, it must exhibit (i) a bimodal distribution of its short-time average kinetic energy in an isoergic simulations, (ii) a rapid increase in the MLE as the solid enters the coexistence region, and (iii) a characteristic two-phase dynamics in the DSF. However, some clusters may exhibit a kind of softening where the system goes continuously from a rigid solidlike state to a floppy liquidlike state without showing any bimodal behavior. The difference between bimodal systems and these depend on the details of the multidimensional potential energy surface. In the following, we discuss the behavior of both DSF's and MLE's in Ar_{17}, a system which does not show bimodality in its short-time kinetic energy distribution.

B. Ar_{17} cluster

In studying Ar_{17}, we first looked at the caloric curve to identify the melting region. The mean temperature T (obtained from the long-time average of the kinetic energy) as a function of the total energy, kinetic plus potential, per atom is shown in Fig. 4. Our results are in agreement with the published results of Beck and co-workers [2] As in Ar_{19}, for low energies, there is a monotonic, linear increase in temperature with energy. At the high energy end of the curve, the increase in temperature is again linear, but with a differ-

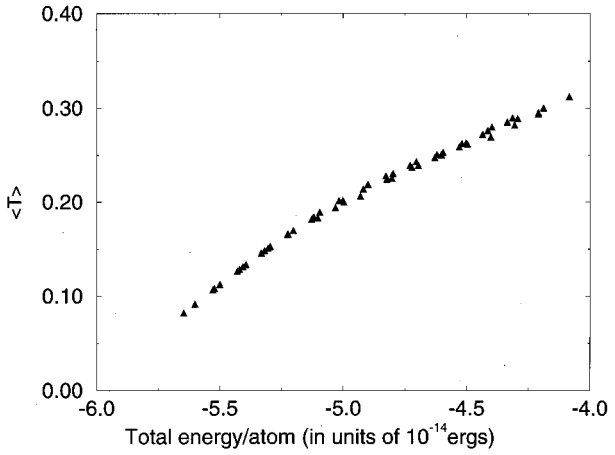

FIG. 4. Temperature (in units of 120 K) vs energy (caloric curve) for Ar_{17}.

ent slope. This corresponds to the nonrigid structure of the cluster. The transition between the rigid and nonrigid forms of Ar_{17} is not clear from looking only at the caloric curve, although one can see a small kink near 20-24K and this transition was characterized by Beck *et. al.* [2] as ''slush-like.'' One way of identifying the transition more precisely is to look at the first and second derivatives of T with respect to E. The other is to study the energy dependence of $F_s(k,t)$, $S_s(k,\omega)$, δ, and λ carefully near the transition region. In addition, one can also look for any multimodal distribution of the short-time averages of the kinetic energy.

In Fig. 5 we give the distribution of the short-time averages of the kinetic energy (averaged over 1000 time steps) for six different values of E starting from deep inside the solid phase through the transition region into the liquid

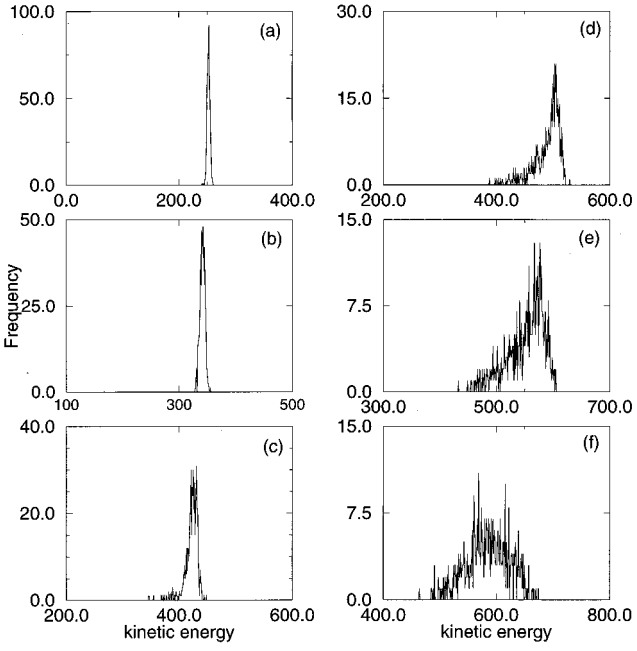

FIG. 5. Distribution of the short time average of the kinetic energy for different values of total energies. (a) -5.5, (b) -5.3, (c) -5.1, (d) -4.9, (e) -4.7, and -4.5 in units of 10^{-14} erg/atom.

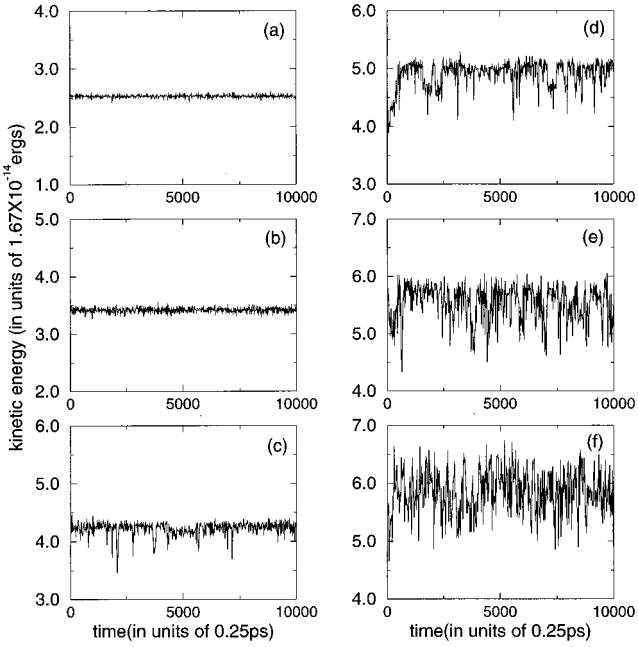

FIG. 6. Kinetic energy as a function of time for the same set of energy values as in Fig. 5.

phase. The transition region is near $E=-5.0\times10^{-14}$ erg/atom. The kinetic energy distribution is unimodal for all the cases, except that below the above energy it is quite sharp but starts to develop a low-energy tail above this value. The origin of the broadening and asymmetry of this distribution comes from dynamic excursion between hot solidlike and cold liquidlike structures. However these structures are not well separated in energy, and the barrier between them is small such that the the cluster makes rapid dynamic excursions between them. These can be easily seen in the time dependence of the kinetic energy given in Fig. 6 for the same values of E.

In Fig. 7, $F_s(k,t)$ is shown for eight different energy values. Since the transition region is not well defined from the caloric curve, we monitored this quantity for more energy values compared to that of Ar_{19}. At $E=-5.1\times10^{-14}$ erg/atom, the cluster displays the characteristics of a rigid structure. The $F_s(k,t)$ saturates to a nonzero value, and small oscillations result from nearly harmonic vibrations of the cluster, and their amplitude increases with k. As the energy is increased, the incoherent inelastic scattering function begins to decay in more or less linear fashion at long times, as we saw in the coexistence region of Ar_{19}. Finally, around $E=-4.4\times10^{-14}$ erg/atom, it displays the characteristics of a nonrigid liquidlike cluster. Thus we see a gradual evolution of the scattering function from that of a rigid to a floppy structure.

In Fig. 8, the dynamic structure factor $S_s(k,\omega)$ is given for the same eight values of the total energy. At the highest energy, $E=-4.4\times10^{-14}$ erg/atom, the curve shows a broadened central peak, the DSF decreasing smoothly with increasing frequency as is characteristic of a nonrigid cluster. As the energy is decreased, the central peak becomes sharper, and a characteristic two-peak structure (see $E=-4.8\times10^{-14}$ erg/atom) develops clearly, reflecting the presence of two different time scales. Finally peaks begin to

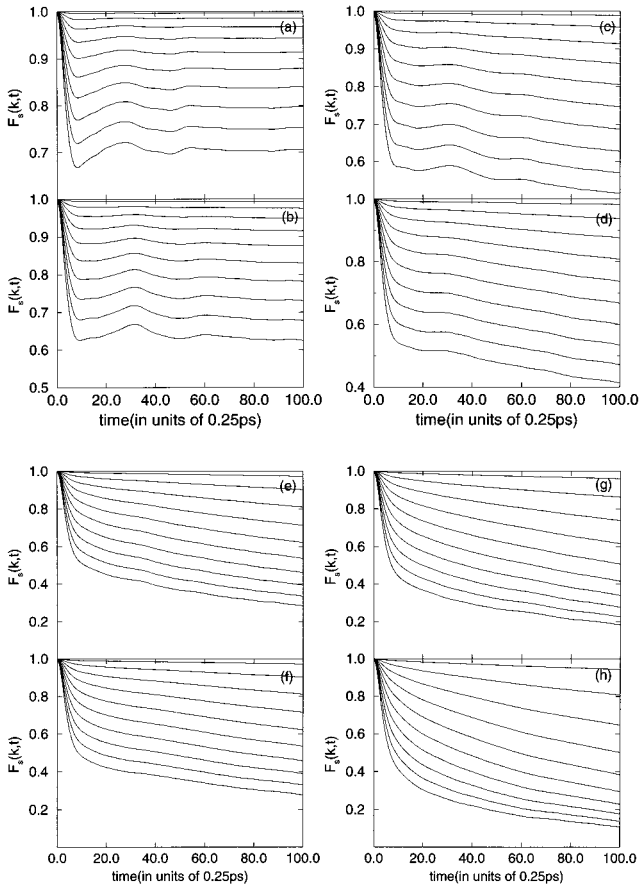

FIG. 7. $F_s(k,t)$ for Ar_{17} is shown for eight energy values (a) -5.1, (b) -5.0, (c) -4.9, (d) -4.8, (e) -4.7, (f) -4.6, (g) -4.5, and (h) -4.4 in units of 10^{-14} erg/atom, as the cluster changes from a rigid solidlike to a nonrigid liquidlike form. The values of k are the same as in Fig. 1.

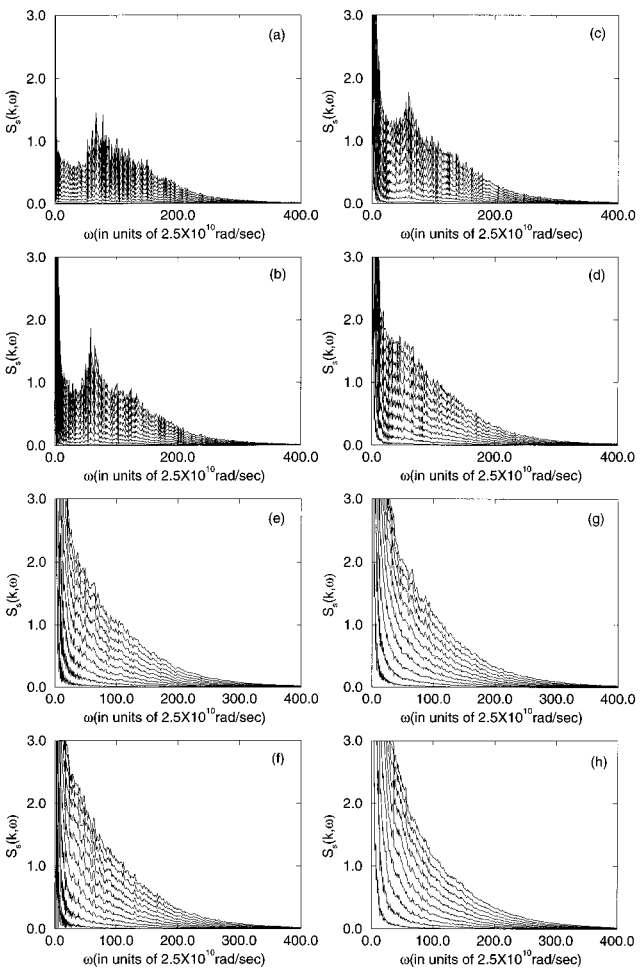

FIG. 8. $F_s(k,\omega)$ for Ar_{17} for the same eight energy values as in Fig. 7 as the cluster changes from a rigid solidlike to a nonrigid liquidlike form. The values of k are the same as in Fig. 1.

form at higher frequencies showing the development of normal modes as the cluster becomes more rigid. Thus the DSF also shows a gradual evolution of the spectral characteristics from a solidlike to liquidlike phase with increasing energy, reflecting what we saw in the scattering function. In examining the scattering function, we find that this function begins to resemble that for Ar_{19} in the coexistence region around $E=-4.8\times10^{-14}$ erg/atom, but is more clear at $E=-4.7\times10^{-14}$ erg/atom. In the dynamic structure factor, this is where the narrow central peak begins to develop.

Figure 9 shows the temperature dependence of MLE for Ar_{17} (squares). One can see from this figure that the MLE increases monotonically, and shows small undulations reflecting the structure of the underlying potential energy surface. At high energies, the liquidlike behavior is confirmed from the DSF (discussed above), diffusion coefficient, bond-length fluctuation [also shown in Fig. 9 (circles)], etc. Suprisingly the bond-length fluctuation δ appears to be still very sensitive and still a good indicator of the transition in this system. In contrast to Ar_{13} and Ar_{19}, where MLE showed a nearly discontinuous jump, it varies rather smoothly across the transition region in Ar_{17}. This behavior can be understood physically as follows. If the cluster has a deep stable minimum and the energy difference between this and the next highest minima is relatively large, and the barrier from both sides is large, then the transition becomes sharp and the cluster is able to show a coexistence of well-defined solidlike and liquidlike forms. This is characteristic of clusters such as Ar_{13} and Ar_{19}. On the other hand, if the

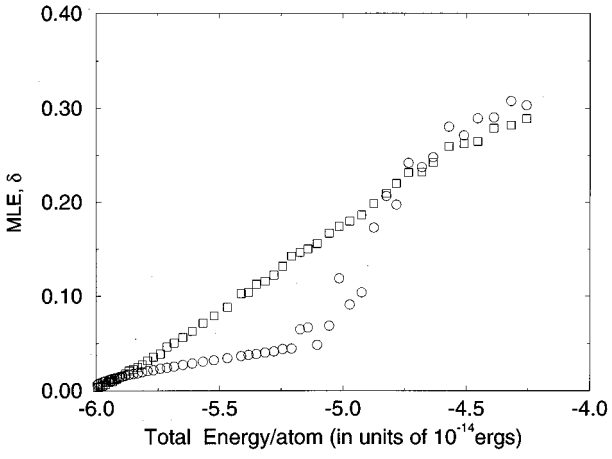

FIG. 9. Average bond length fluctuation (circles) and MLE as a function of energy (squares) for an Ar_{17} cluster. The behavior of MLE is rather smooth.

cluster has a large number of isomers close in energy and the barriers between these isomeric states are not large, then the cluster samples these isomers during the simulation and the transition becomes smooth. The cluster does not show any kind of bimodality. This is the case for clusters like Ar_{17}. In these clusters the access to the phase space volume with energy is rather gradual, and hence the MLE and other dynamic indicators do not show any sharp change in their behavior across the transition.

V. SUMMARY

In summary, we extended our earlier MD simulation studies of DSF and MLE for Ar_{13} to Ar_{19} and Ar_{17} clusters to investigate the transition from the low-energy solidlike to high-energy liquidlike structures. We find that both MLE and the DSF remain good indicators characterizing the transition region. The energy dependence of the MLE shows different characteristics for clusters with a coexistence transition region and those without one. In the case of the former, MLE shows a rapid increase near E_f as the cluster enters the coexistence region from below, i.e., when the rigid but anharmonic clusters begins to sample the liquidlike phase space. MLE does not show any significant feature near E_m when the cluster leaves the coexistence region and goes into a liquidlike phase. In the case of clusters showing a slushlike transition, MLE changes smoothly across the transition. In contrast to the MLE, we find that DSF shows similar behavior for both types of transitions, namely, signatures of both solidlike and liquidlike dynamics co-existing at the same energy.

ACKNOWLEDGMENTS

This work was partially supported by NSF Grant Nos. CHE9224102 and CHE9633798, and the Center for Fundamental Materials Research at Michigan State University. G.T. acknowledges a summer REU support (funded by NSF) at Michigan State University. S.K.N. would like to acknowledge partial support from the Department of Energy.

[1] R. P. Andres, R. S. Averback, W. L. Brown, L. E. Brus, W. A. Goddard III, A. Kaldor, S. G. Louie, M. Moscovits, P. S. Peercy, S. J. Riley, R. W. Siegel, f. Spaepen, and Y. Wang, J. Mater. Res **4**, 704 (1989).

[2] R. S. Berry, in *Physics and Chemistry of Finite Systems; From Clusters to Crystals*, Vol. 374 of *NATO Advanced Study Institute, edited by P. Jena, S. Khanna, and B. K. Rao, (Kluwer Academic, Norwek, MA, 1992); T. L. Beck, J. Jellinek, and R. S. Berry, J. Chem. Phys.* **87**, 545 (1987); D. J. Wells and R. S. Berry, Phys. Rev. Lett. **73**, 2875 (1994); T. L. Beck, D. M. Leitner, and R. S. Berry, J. Chem. Phys. **89**,1681 (1993); T. L. Beck and R. S. Berry, *ibid*. **88**, 3910 (1993); H. L. Davis, J. Jellinek, and R. S. Berry, *ibid*. **86**, 6456 (1987).

[3] C. L. Briant and J .J. Burton, J. Chem. Phys. **63**, 2045 (1975).

[4] S. K. Nayak, R. Ramaswamy, and C. Chakravarty, Phys. Rev. E **51**, 3376 (1995).

[5] S. K. Nayak, R. Ramaswamy, and C. Chakravarty, Phys. Rev. Lett. **74**, 4181 (1995).

[6] D. Leitner, R. S. Berry, and R. M. Whitnell, J. Chem. Phys. **91**, 3470 (1989); R. J. Hinde, R. S. Berry, and D. J. Wales, *ibid.* **96**, 1376 (1992); C. Amitrano and R. S. Berry, Phys. Rev. Lett. **68**, 729 (1992); Phys. Rev. E **47**, 3158 (1993).

[7] A. Bhattacharya, B. Chen, and S. D. Mahanti, Phys. Rev. E **53**, R33 (1996).

[8] J. Jellinek, T. L. Beck, and R. S. Berry, J. Chem. Phys. **84**, 2783 (1986).

[9] V. Mehra and R. Ramaswamy, Phys. Rev. E **53**, 3420 (1996).

[10] P. Butera and G. Caravati, Phys. Rev. A **36**, 962 (1987).

[11] For a review of interesting developments in the field, see *Simulations of Liquids and Solids*, edited by G. Ciccotti, D. Frenkel, and I. R. McDonald (North-Holland, Amsterdam, 1987).

[12] M. P. Allen and D. J. Tildesley, *Computer Simulation of Liquids* (Clarendon, Oxford, 1993).

[13] J. M. Haile, *Molecular Dynamics Simulation: Elementary Methods* (Wiley, New York, 1992).

[14] G. Benettin, L. Galgani, and J-M Strelcyn, Phys. Rev. A **14**, 2338 (1976).

[15] H. D. Mayer, J. Chem. Phys. **84**, 3147 (1986).

[16] H. Seong and S. D. Mahanti, Phys. Rev. B **49**, 5042 (1994), H. Seong, Ph.D thesis, Michigan State University, 1993.

[17] S. K. Nayak, P. Jena, K. D. Ball, and R. S. Berry (unpublished).